

The influence of Sr and H₃PO₄ concentration on the hydration of SrCaHA bone cement

Dagang Guo · Mengmeng Mao · Wenli Qi ·
Hongyuan Li · Pengfei Ni · Guohan Gao ·
Kewei Xu

Received: 18 February 2011 / Accepted: 13 September 2011 / Published online: 7 October 2011
© Springer Science+Business Media, LLC 2011

Abstract Sr-contained calcium hydroxyapatite (SrCaHA) cement is a potential biomaterial for in vivo bone repair and surgery fixation due to its excellent biodegradability, bioactivity, biocompatibility, easily shaping and self-hardening. We had ever reported the in vitro physiochemical properties, biocompatibility and in vivo degradability of the SrCaHA cement obtained by mixing a cement powder of Ca₄(PO₄)₂O/CaHPO₄/SrHPO₄ and a cement liquid of diluted H₃PO₄ aqueous solution. In the present study, we intensively studied the influences of both Sr content and H₃PO₄ concentration in diluted phosphoric acid aqueous solution on the setting time, hydration heat-liberation behaviours, and real-time microstructure and phase evolutions of the SrCaHA cement. The results show that both PO₄³⁻ and H⁺ ions in PA solution attended the hydration reaction as reactants, and thus the increase of the PA concentration not only promoted the dissolution of Ca₄(PO₄)₂O but also pushed the hydration progress of SrCaHA bone cement. Sr content exhibits a remarkable retardation role on the apatite transformation of the SrCaHA cement pastes which probably attributed to its higher degree of supersaturation for yielding apatite crystals and lower transformation rate when exposed to the Sr²⁺-containing hydration system. This present results contribute to a better understanding on the hydration mechanism of the new SrCaHA cement and help to the more precisely controlling of its hydration process.

1 Introduction

Hydroxyapatite or calcium hydroxyapatite (CaHA), in forms of powder (or particles), ceramics, bone cement and bone tissue engineering scaffold, is such a biomaterial which has been studied so far most deeply in lab and also applied most broadly in clinic. However, the most critical disadvantage for this kind of apatite-based biomaterials is their low degradation rate in vivo which is too slow to meet the faster new bone growth rate. The strategy of substitution of strontium (Sr) to calcium in hydroxyapatite is quite effective to increase its degradation rate [1]. Moreover, this Sr-incorporating approach also significantly improves its biocompatibility [2], bioactivity [3], osteoconduction [2], compressive strength [4] and other biological effects on human bone [5, 6]. In the recent years, strontium-incorporated hydroxyapatite bone cement (SrCaHAC) has been intensively studied, and various SrCaHAC systems have been developed, such as Ca₄(PO₄)₂O/ α -Ca₃(PO₄)₂ system [7], α -Ca₃(PO₄)₂/SrCO₃/Ca(H₂PO₄)₂·H₂O system [8], Ca₄(PO₄)₂O/CaHPO₄/SrHPO₄ system [4, 9] and SrCaHA/resin composite bone cement [10], etc. Especially, we had ever developed the Ca₄(PO₄)₂O/CaHPO₄/SrHPO₄ system and demonstrated this SrCaHAC possessed a high compressive strength, controllable degradation rate, and a suitable acid–base degree of its initial cement pastes and almost no harmful impurity could be detected in its final hardened product by a series of in vivo and in vitro experiments [4, 9].

In our previous studies [11], it is was also found that the Ca₄(PO₄)₂O/CaHPO₄/SrHPO₄ powder mixture was not capable of being hydrated in the cement liquids such as de-ionized water, pure acidic solution (e.g. C₆H₈O₇·H₂O, CA) and Na⁺- or Cl⁻-containing solution, but could be partly hydrated in the neutral PO₄³⁻-contained solution (e.g. Na_xH_{3-x}PO₄, NPS) and completely hydrated in the acidic PO₄³⁻-contained

D. Guo (✉) · M. Mao · W. Qi · H. Li · P. Ni · G. Gao · K. Xu
State Key Laboratory for Mechanical Behavior of Materials,
School of Material Science and Engineering, Xi'an Jiaotong
University, Xi'an 710049, China
e-mail: guodagang@mail.xjtu.edu.cn

K. Xu
Xi'an University of Arts and Science, Xi'an 710065, China

solution (i.e. H_3PO_4 aqueous solution, PA) with a higher concentration. It was speculated that both the PO_4^{3-} ion and the acidity of the cement liquid might be the most essential hydration preconditions for the $\text{Ca}_4(\text{PO}_4)_2\text{O}/\text{CaHPO}_4/\text{SrHPO}_4$ system SrCaHAC paste. However, this speculation needed to be further confirmed and interpreted. Certainly, the difference presented in the hydration preconditions between the Sr-containing CPC and Sr-free CPC was caused by the incorporation of Sr into CPC powder. This suggests that Sr should play an important role in the hydration process of CPC or the transformation of CaHA. Therefore, in order to confirm and interpret this speculation and also get a better understanding on the hydration mechanism of this SrCaHAC, the present work intensively investigated the influences of both Sr content ($\text{Sr}/(\text{Sr} + \text{Ca})100\%$) in cement powder and H_3PO_4 concentration in cement liquid on their basic hydration properties, including setting time, hydration heat-liberation behaviours, and real-time microstructure and phase evolutions of this SrCaHAC.

2 Experiments and methods

2.1 Material preparation

The solid phase powders of the SrCaHAC are composed of tetracalcium phosphate ($\text{Ca}_4(\text{PO}_4)_2\text{O}$, TTCP), dicalcium phosphate anhydrous (CaHPO_4 , DCPA) and strontium hydrogen phosphate (SrHPO_4 , DSPA) [4]. $\text{Ca}_4(\text{PO}_4)_2\text{O}$ was prepared by heating a mixture of dicalcium phosphate (DCPD, $\text{CaHPO}_4 \cdot \text{H}_2\text{O}$) and calcium carbonate (CC, CaCO_3) with an equivalent molar ratio. This mixed precursors with a Ca/P molar ratio of 2.0 were continuously heated up to 1500°C and maintained 10 h at least in an air furnace with silicomolybdc rods as heating units. The obtained products were then quenched to room temperature in a desiccator. After crushed by mortar and pestle, the product was wetly ground in a ball mill for more than 10 h with absolute ethyl alcohol as a grinding medium. DCPA was prepared by heating commercial DCPD at 110°C for more than 48 h and then grounded by the above similar ball milling routes. DSPA was synthesized with the similar precipitation method reported elsewhere [12], where the precursors of $\text{Sr}(\text{NO}_3)_2$ and $(\text{NH}_4)\text{HPO}_4$ were mixed at pH 7.0 with an equivalent molar ratio. The deposited sediments were centrifugally washed for more than 3 times by using absolute ethyl alcohol and then dried in oven at 80°C for at least 10 h. All these reagents used in the present experiments were purchased from Sinopharm Chemical Reagent Co., Ltd., China. The milling conditions were described as follows: the materials of ball and jar (200 ml in volume) were aluminum oxide (Al_2O_3) and nylon, respectively; 100 smaller balls in $\Phi 5$ and 15 larger

balls in $\Phi 10$ were used for each jar and generally the total mass and average particle size of the raw powders for each jar were 50 g and 30–50 μm , respectively; the rotation speed was set at 400 rpm (r/min). The device used here was planet ball-milling machine produced by Nanjing Uni. Instrument Co., China. The particle distribution data of various cement powder components, measured with the light scattering particle size analyzer (Winner 2000, Jinan Instrument Co., China), were shown in Table 1. In the present study, two SrCaHAC pastes including 5%Sr-contained CaHAC (5%SrCaHAC) and 10%Sr-contained HAC (10%SrCaHAC) had been investigated and the Sr-free HAC (0%SrCaHAC) was used as a control. The molar numbers of phosphate salts and the corresponding Sr doses in various cement powder mixtures were summarized in Table 2. In addition, the cement liquids used for preparing the SrCaHAC pastes (5%SrCaHAC, 10%SrCaHAC) and the Sr-free CaHAC pastes (0%SrCaHAC) were 1.0 M H_3PO_4 solution (PA) and de-ionized water, respectively.

2.2 Hydration heat-liberation curves tests

The weights of both the cement powder and the cement liquid used in this experiment were 0.7282 ± 0.0001 and 0.4855 ± 0.0001 g, respectively. The weight ratio of the cement powder to the cement liquid (P/L) was 1:1.5. The hydration heat-liberation behaviors of the SrCaHAC or Sr-free CaHAC pastes were measured by using the microcalorimeter (RD496-III, CAEP, China). In order to control the starting time of the hydration reaction, a glass isolator loaded with the cement liquid above the cement powder was specially designed to ensure the cement powder complete isolation from the cement liquid before the hydration reaction started. When the heat equilibrium reached, the bottom of the glass isolator was carefully punctured using a long stainless steel needle and the cement liquid flowed into the cement powder loaded at the bottom of the sample cell, and then the hydration reaction started. It should be pointed out that the bottom of the glass isolator was made thin enough to be easily punctured and a glass mesh screen was placed somewhere between the glass isolator and bottom of the sample cell to collect the broken glass pieces. The hydration temperature was preset at 310.15 ± 0.005 K and the corresponding calorimetric constants decided by the Joule effect experiment were $64.538 \pm 0.038 \mu\text{V mW}^{-1}$. Both the accuracy and the precision of the apparatus were adjusted by measuring the dissolving enthalpy of analytically pure potassium chloride in de-ionized water. In the present study, the termination time of the hydration reaction was decided by appearance of a long zero-value line on the heat-liberation curve.

Table 1 Particle size distributions in cement powder components of SrCaHAC in various grounded conditions

Samples		Grounding time (h)	D25	D50	D75	D90	Dav.	S V ⁻¹ (cm ² cm ⁻³)
Components	Code							
TTCP1	T1	72 h	1.77	2.58	6.03	11.13	4.79	24199.33
TTCP2	T2	10 h	1.89	3.05	16.12	48.09	13.0	18737.91
TTCP3	T3	0 h, 400# ^a	9.93	23.86	39.25	52.55	26.42	5797.68
DCPA0	D0	48 h	1.43	1.78	2.19	2.59	1.83	36161.08
DSPA1	S1	72 h	1.38	1.75	2.17	2.59	1.84	36925.73
DSPA2	S2	48 h	1.50	1.98	5.43	12.47	4.76	24478.25
DSPA3	S3	1 h	1.64	2.27	9.35	24.34	7.51	25418.64

^a Denotes the powder was sieved through a # 400 mesh ASTM sieve after manual grounding

Table 2 The cement powder composition of SrCaHAC with various Sr contents

Samples		TTCP (mol)	DCPA (mol)	DSPA (mol)	Sr/(Sr + Ca) (%)
0%Sr-HAC	C0	1.0x ^a	1.0x	0x	0
5%Sr-HAC	C1	1.0x	0.75x	0.25x	5
10%Sr-HAC	C2	1.0x	0.50x	0.50x	10

^a 1.0x denotes the molar number of one phase in SrCaHAC powder, x is variable; C0, C1, C2, denote 0% SrCaHAC, 5% SrCaHAC, 10% SrCa AC, respectively

2.3 Setting time tests

The setting times, including the initial time (t_i) and the final time (t_f), of various cements were determined using Gilmore needles according to the C266-89 ASTM standard as described elsewhere [13]. In this method, the tested cement samples were maintained at 37°C with a relative humidity of 100%. The processing details of the sample for testing the setting times were described as follows: the cement pastes were first prepared by mixing the cement powder and the diluted phosphoric acid solution (PA, 0.5–1.50 M, M = mol/l) with a certain weight ratio using a spatula; after mixed for 30 s, the cement pastes were placed into a quartz glass mold (6 mm × 12 mm in diameter and height) with a pressure of 0.70 MPa and then immediately stored in a 100% relative humidity incubator at 37°C; at the preset time, the cement pastes were taken out for testing their setting times. Generally, six parallel tests were used to obtain the mean value and standard variance for each sample. The apparatus used here was the Cement Standard Consistency & Setting Time Device (Lu-Xun Co., China).

2.4 X-ray diffraction (XRD) pattern determinations

The processing details of cement samples for determining the following XRD patterns were the same to those of the cement samples for the setting time tests.

2.4.1 Various SrCaHAC pastes formed from different cement liquids

To demonstrate the roles of both PO₄³⁻ ion and acidity of the PA cement liquid on the hydration reaction of the SrCaHAC pastes, the XRD patterns of various SrCaHAC pastes (T₂S₁D₀–C₂) formed from different cement liquids were determined by an XRD device with Cu-K_α radiation and Ni filter. The cement liquids used here included PO₄³⁻ containing solutions (e.g. 0.5–1.0 M sodium hydrogen phosphate (Na_xH_{3-x}PO₄) solutions and 0.1–0.75 M H₃PO₄ solutions), PO₄³⁻-free solutions (e.g. 0.9%NaCl solution, de-ionized water and 0.5–1.0 M citrate acid), neutral solutions (0.5–1.0 M sodium hydrogen phosphate, 0.9%NaCl solution, de-ionized water) and acidic solutions (0.5–1.0 M citrate acid, 0.1–0.75 M H₃PO₄ solution). The electrical voltage and current used here were 35 kV and 30 mA, respectively.

2.4.2 Real-time phase evolutions of several SrCaHAC pastes

To investigate the influences of both Sr dose and H₃PO₄ concentration on the transformation rate of apatite, the real-time XRD patterns of the 10%SrCaHAC pastes (powder: T₂S₃D₀–C₂; H₃PO₄ concentration: 1.0 mol/l) and the 0% SrCaHAC pastes (powder: T₂D₀–C₀; H₃PO₄ concentration:

0.5 or 1.0 mol/L) obtained at different hydration time (15 min–24 h) were determined by an XRD apparatus. The apparatus parameters for measuring the X-ray patterns were the same to those mentioned in Sect. 2.4.1.

2.5 Calculation of the apatite transformation ratio and real-time microstructure evolutions

By contrast with the hydration heat-liberation behaviors mentioned above, the real-time phase evolutions of the 5%SrCaHAC (powder: T₂S₁D₀-C₁; H₃PO₄ concentration: 0.75 M) paste at various hydration times were determined by an XRD with Cu-K_α radiation and Ni filter. In order to immediately terminate the hydration reaction at one preset time, the tested cement paste was taken out of the incubator and then quickly immersed into refrigerated acetone at -16°C. To calculate the apatite transformation ratio, a calculation formula had been proposed on the conventional CaHAC (Ca₄(PO₄)₂O/CaHPO₄) [14]. In the present study, we made a suitable modification on this formula due to the cement composition difference of hydration system. The modified formula corresponding to T₂S₁D₀-C₁ is described as Eq. (1),

$$a_t = \frac{\frac{AP_t}{AP_\infty} + 0.5 \times \left[1 - \frac{TTCP_t}{TTCP_0} + 0.75 \times \left(1 - \frac{DCPA_t}{DCPA_0} \right) + 0.25 \times \left(1 - \frac{DSPA_t}{DSPA_0} \right) \right]}{2} \quad (1)$$

where, a_t is the transformation ratio of apatite at hydration time t ; $TTCP_0$, $DCPA_0$ and $DSPA_0$ are integral areas corresponding to the main diffraction peaks of TTCP, DCPA and DSPA, respectively, in the original cement powder before hydration; $TTCP_t$, $DCPA_t$ and $DSPA_t$ are integral areas corresponding to the same main diffraction peaks of TTCP, DCPA and DSPA, respectively, at hydration time t ; AP_t and AP_∞ are integral areas corresponding to the main diffraction peak of the newly transformed apatite (AP) at hydration time t and the termination time, respectively. The diffraction peaks referred here are 29.2° (032) and 29.8° (040) for TTCP, 26.6° (110) for DCPA, 25.9° (002) for AP, and 24.4° and 24.8° for DSPA, respectively. The diffraction peak of apatite located at 25.9° (002) was selected for the above integral calculation instead of the highest diffraction intensity peak located at 31.77° (211) only based on the consideration that the crystallinity of the hydration apatite was weak and the former diffraction peak was more easily identified than the latter one.

In the present experiments, the tested cement samples were divided into two groups under the same processing conditions: one group was used to determine their XRD patterns and the

other was used to examine their microstructures by using scanning electron microscopy (SEM, S-2700, Japan). The processing details of these samples were the same to those used to test the setting times mentioned above.

3 Results

3.1 Effect of PA concentration and Sr²⁺ ion on the hydration process

Figure 1 shows the setting times (t_I , t_F) curves of both the 10%SrCaHAC (T₁S₂D₀-C₂) paste and the 0%SrCaHAC (T₁D₀-C₀) paste in the diluted phosphoric acid (PA) with different concentrations. In this experiment, the P/L mass ratio and the hydration temperature for each cement paste were kept at 1.8 and 37°C, respectively. It was noted that both the setting time (t_I and t_F) of the 10%SrCaHAC paste and the 0%SrCaHAC paste gradually decreased as the PA concentration increased (see Fig. 1). It indicates H₃PO₄ in the cement liquid works as a setting accelerator whatever for 10%SrCaHAC paste or the 0%SrCaHAC paste. Comparatively, both t_I and t_F of the 10%SrCaHAC paste were

significantly slower than those of the 0%SrCaHAC paste formed from the PA cement liquids with the same concentration. It implies that the incorporation of strontium ion or strontium-containing salt into the CaHAC paste delays its hydration reaction.

Figure 2 shows the hydration heat-liberation characteristic curves of both the 10%SrCaHAC (T₁S₁D₀-C₂) paste and the 0%SrCaHAC (T₁D₀-C₀) paste in different cement liquids. The hydration heat-liberation curve of the 0%SrCaHAC paste in the de-ionised water extremely approaches to the typical hydration heat-liberation curve of the Portland cement [15]. This kind of curve could be divided into five typical periods (see Fig. 2a): the starting or physical wetting period (A), induction or latency periods (B), acceleration period (C), deceleration period (D) and termination period (E). Both the typical periods of the 0%SrCaHAC paste in the de-ionised water and its maximal heat-liberation rates were extremely similar to those reported elsewhere [16]. However, surprisingly, the induction period (B) here could be traced more than 30 h, much longer than the corresponding time (~30 min) of another Sr-free CaHAC paste reported in the above same

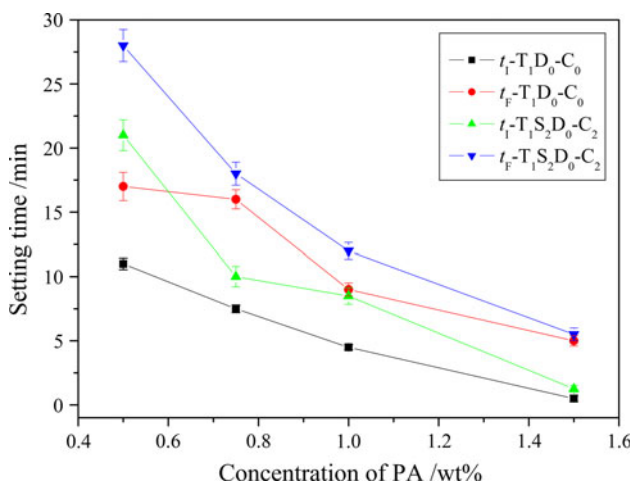
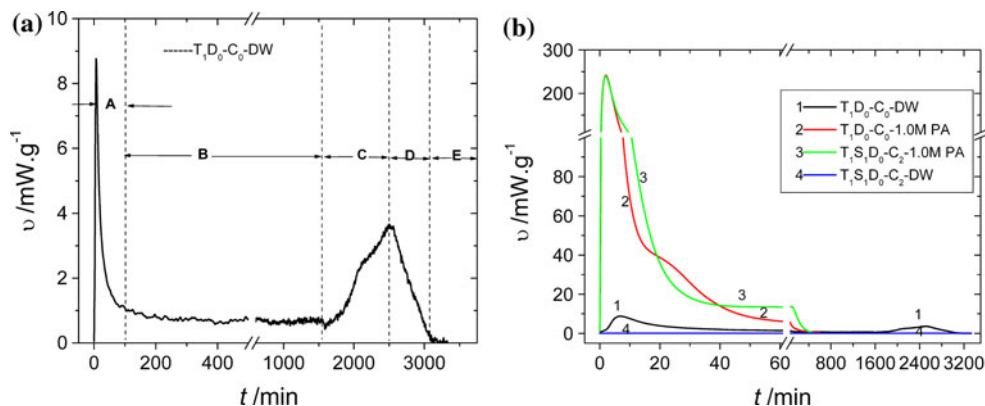


Fig. 1 Effect of the PA concentration on the setting time of 0%SrCaHAC paste (T₁D₀-C₀) and 10%SrCaHAC paste (T₁S₂D₀-C₂)

literature. By contrast, the hydration heat-liberation curve of the 10%SrCaHAC paste in de-ionised water was basically a Zero-value curve (see curve “4” in Fig. 2b) that means no reaction happens, well consistent with the result obtained from XRD analysis reported previously [11] where no new diffraction peak could be detected. This result further indicates the presence of the SrHPO₄ salt or Sr²⁺ ion in the CaHAC paste strongly suppresses the hydration reaction of the Ca₄(PO₄)₂O/CaHPO₄ mixture exposed in the de-ionised water. However, when using the 1.0 M PA solution as the cement liquid, the hydration heat-liberation characteristic curves of both the 10%SrCaHAC paste (see curve “3” in Fig. 2b) and the 0%SrCaHAC paste (see curve “2” in Fig. 2b) were significantly different. In comparison with the case in the deionized water, the hydration heat-liberation rate of the 10%SrCaHAC paste in 1.0 M PA solution was strongly increased, which led to an obvious overlap appeared between the starting period and the acceleration period instead of the induction period. The maximal heat-liberation rates of both the 10%SrCaHAC paste and 0%SrCaHAC paste in 1.0 M PA solution almost increased to 250 mW/g, approximately 27 times higher

Fig. 2 The typical five stages of hydration heat-liberation rate curve of **a** T₁D₀-C₀ powders in DW, and **b** the heat-liberation rate curves of T₁D₀-C₀ and T₁S₁D₀-C₂ powders in both DW and 1.0 M PA



than that of the 0%HAC paste in the deionized water under the same testing conditions [16]. Furthermore, the maximal heat-liberation rate peak of the 10%SrCaHAC paste emerged at just 2 min after the hydration reaction started, and then the deceleration period almost ended at 50 min. About 70% of the total hydration heat had been liberated within the first 50 min. It clearly indicates selecting the 1.0 M PA as the cement setting liquid instead of the deionized water greatly accelerated the hydration reaction of the SrCaHAC paste and shortened the reaction time.

Figure 3 shows the real-time XRD patterns of the 10%SrCaHAC (T₂S₃D₀-C₂) paste and the 0%SrCaHAC (T₂D₀-C₀) paste in the PA solution with different concentrations. As we reported previously [4, 11, 17], the hydration products of the Ca₄(PO₄)₂O/CaHPO₄/SrHPO₄ system cements had been testified as SrCaHAC phases by both the shifting of XRD peaks and variations of cell parameter values. In the 0.5 M PA solution (see Fig. 3a), no new diffraction peak but those of the original cement powders were detected in the 10%SrCaHAC paste during the whole tested hydration time from 15 min to 24 h. However, in the 1.0 M PA solution, the diffraction peaks of the 10%SrCaHAC paste hydrated over 15 h were similar to those of pure apatite. It indicates that increasing the PA concentration significantly accelerates the hydration reaction or enhances the transformation rate of apatite, well consistent with the corresponding hydration heat-liberation result mentioned above. Interestingly, the 0%SrCaHAC paste only needed 6 h to complete the transformation of apatite in 1.0 M PA solution (see Fig. 3c), which is largely shorten by contrast with the corresponding time (i.e. 15 h) for the 10%SrCaHAC paste under the same conditions. This result intuitively confirms that Sr²⁺ plays an important retarding role in the hydration of the SrCaHAC paste.

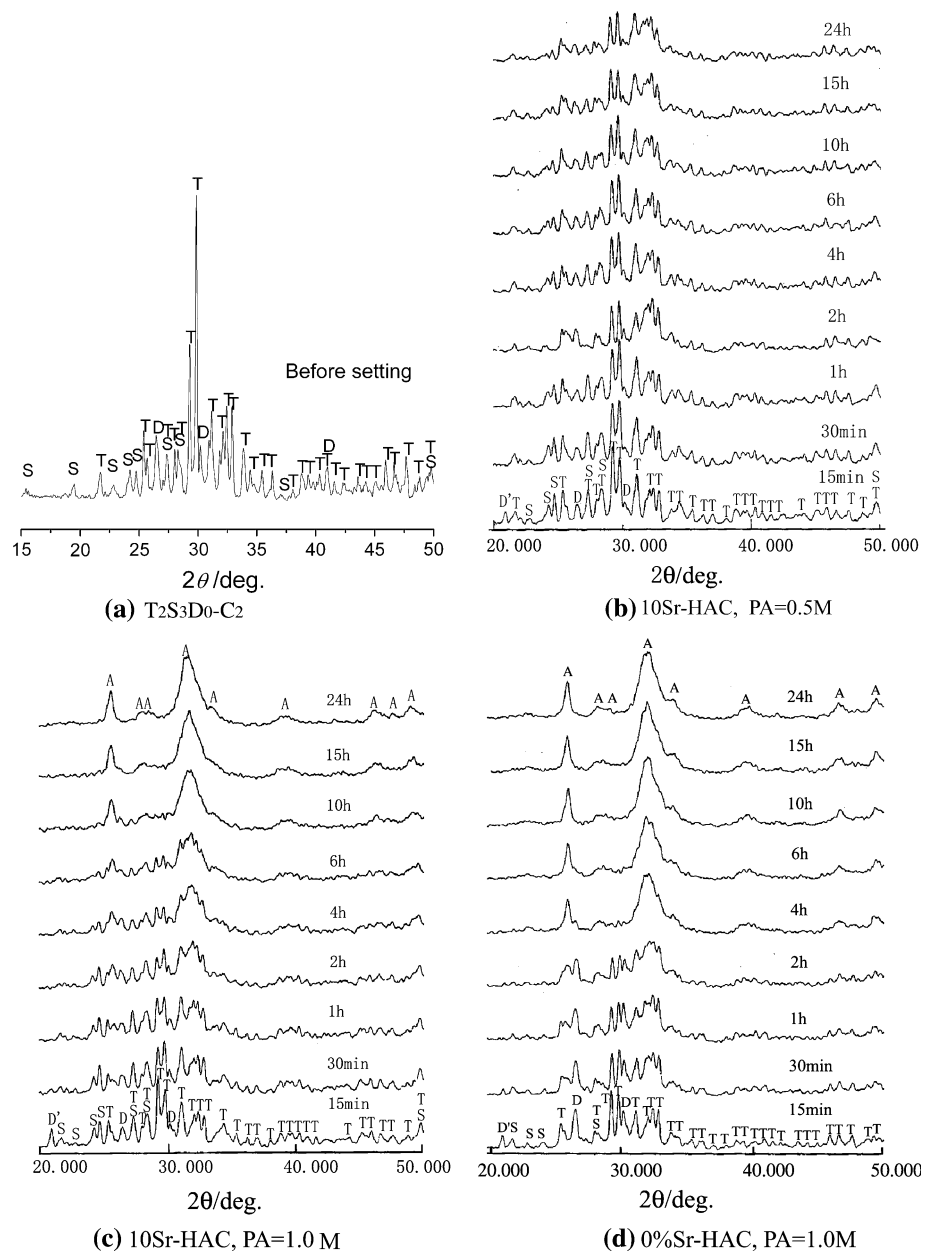
3.2 Composition variations and microstructure evolutions

Figure 4 shows the XRD patterns of the 5%SrCaHAC (T₃S₁D₀-C₁) paste at various hydration stages after mixed

with the 1.0 M PA cement liquid. Basically, other than diffraction peaks of the original reactants, only those corresponding to Sr-contained hydroxyapatite (SrCaHA) [4] (major hydration products) and dicalcium phosphate dihydrate ($\text{CaHPO}_4 \cdot 2\text{H}_2\text{O}$, DCPD, minor flake intermediate products) were detected during the hydration process of the SrCaHAC paste from the starting time to 24 h. Interestingly, the main diffraction peaks of $\text{CaHPO}_4 \cdot 2\text{H}_2\text{O}$ located at $2\theta = 12^\circ$ and $2\theta = 21^\circ$, respectively, could be detected only in the very early hydration stages (15 min–1 h) and then disappeared beyond 2 h. When the hydration time was further prolonged to 48 h, the hydration products were basically pure SrCaHA. Figure 5 shows the typical

SEM photographs in the fractured surfaces of the hardened cement samples at various hydration stages. Before hydration reaction beginning (see Fig. 5a), the cement powders were observed like a complex of large particles (i.e. TTCP) loosely wrapped by many small particles (i.e. DCPA and DSPA). When the hydration time lasted to 15 min, these small particles were found to tightly bind the surface of the large particles (see Fig. 5b), suggesting a slight hydration reaction started. At 30 min, these loose particles had been coagulated together (see Fig. 5c). Interestingly, some sheet-like crystals could be clearly observed to bridge the inwalls of macropores, which actually were the air poles formed from processing step of

Fig. 3 **a** The XRD pattern of the starting 10%SrCaHAC powders ($\text{T}_2\text{S}_3\text{D}_0\text{-C}_2$) and the real-time XRD patterns of 10%SrCaHAC powders ($\text{T}_2\text{S}_3\text{D}_0\text{-C}_2$) mixed with **b** 0.5 M PA and **c** 1.0 M PA, respectively, and **d** that of 0%SrCaHAC ($\text{T}_2\text{D}_0\text{-C}_0$) powders mixed with 1.0 M PA. All samples were stored under conditions of an atmosphere of 37°C and a 100% relative humidity for 24 h



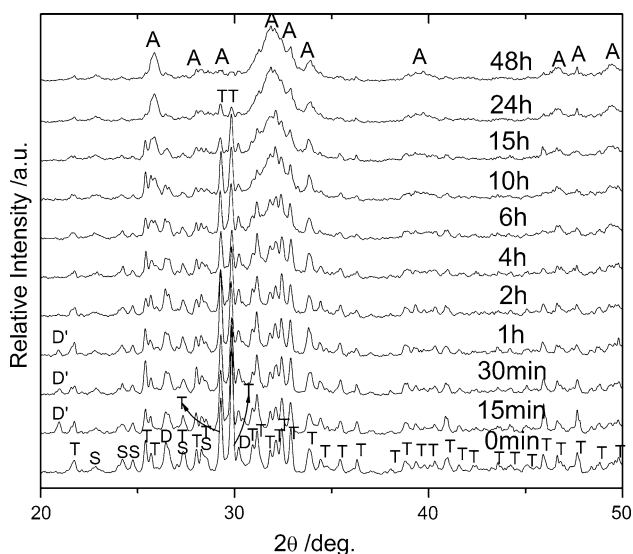


Fig. 4 The real-time XRD patterns of the $(T_3S_1D_0-C_1)$ 10% SrCaHAC powders after mixed in 1.0 MPA (D' DCPD; D DCPA; S DSPA; A SrCaHA; T TTCP)

CPC samples, in the cement sample (see Fig. 5c, d). Combined with the above XRD analysis shown in Fig. 4, these sheet-like crystals were $CaHPO_4 \cdot 2H_2O$, the sole immediate hydration product of DCPA. Beyond 1 h, these sheet-like crystals were basically disappeared and the structure of the hydrated cement samples gradually turned more compact. When extending the hydration time more than 24 h, a layer of chrysanthemum petal-like crystals appeared (see Fig. 5k, l), probably formed from the dissolving and recrystallizing process of apatite in SBF [4].

Figure 6 shows the transformation percentages of the SrCaHA product and the remained molar percentages (RMPs) of respective phosphate salt reactants in the 5% SrCaHAC $(T_3S_1D_0-C_1)$ paste at various hydration time. From the beginning to 2 h, all the RMPs of $Ca_4(PO_4)_2O$, $CaHPO_4$ and $SrHPO_4$ in the cement paste decreased rapidly and the decreasing rate of the former one is slightly faster than those of the latter two. As a result, a rapid increase could be observed on the transformation percentage curves of SrCaHA. It indicates that $Ca_4(PO_4)_2O$ exhibits the fastest hydration rate among all reactants in the very initial hydration stages and thus led to a rapid increase in the transformation ratio of apatite. 2 h later, the RMP slope of $Ca_4(PO_4)_2O$ suddenly decreased as well as those of $CaHPO_4$ and $SrHPO_4$, resulting in a corresponding variation on the transformation percentage curves of SrCaHA. From 4 to 24 h, all the RMPs of $Ca_4(PO_4)_2O$, $SrHPO_4$ and $CaHPO_4$ maintained comparatively stable decreasing rates, and similar variation was also observed on the transformation percentage curve of SrCaHA. Finally, $SrHPO_4$ firstly completed its hydration at 15 h, while both $Ca_4(PO_4)_2O$ and $CaHPO_4$ completed their reaction till 48 h.

4 Discussions

The setting time (t_i , t_F) is an important property for bone cement which involves the optimum clinical operation time [18]. It also reflects the status of hydration reaction in the very initial stages, conventionally relating to several or tens of minutes after the hydration reaction begins. Differently, both the hydration heat-literature behaviors and the phase evolutions exhibit the whole hydration reaction behaviors or characteristics from the very beginning to the preset setting time. Summarized from the results shown in Figs. 1, 2, 3, increasing the PA concentration not only significantly shortened both t_i and t_F but also increased the hydration rate of the cement powders and transformation of apatite as well. Especially, the 1.0 M PA largely shortened the induction period or latency period of both Sr-free or Sr-containing HAC pastes compared with the case when the cement pastes were exposed in de-ionized water. As a result, an obvious overlap was observed between the starting period and the acceleration period instead of the induction period. Undoubtedly, the PA concentration was one of critical parameters for the hydration of the $Ca_4(PO_4)_2O/CaHPO_4/SrHPO_4$ system cement confirmed by the above results. Its influence mechanism could be understood as the following two aspects. First, once the cement powders met with the stronger acidic PA cement liquid in the very early stage of hydration, the sole alkaline phosphate salt, $Ca_4(PO_4)_2O$, fiercely dissolved and synchronously the pH value of the hydration system immediately rose [4], which results in the rapid hydration of the acidic cement powder. Therefore, when further enhancing the PA concentration, both the hydration rate of $Ca_4(PO_4)_2O$ and the later transformation rate of SrCaHA was increased. Second, from the viewpoint of chemical balance, both PO_4^{3-} and H^+ attended the hydration reaction acted as the reactants (see the following Eqs. 3–4). As a result, increasing the PA concentration pushed the chemical balance of the hydration reaction towards formation of SrCaHA product, which enhanced the hydration yield.

Based on the phase evolution result obtained from Fig. 4, the sole intermediate phase, $CaHPO_4 \cdot 2H_2O$ (DCPD), formed at 15 min and simultaneously both the diffraction peak intensities of $CaHPO_4$ and $Ca_4(PO_4)_2O$ slightly decreased. The intermediate phase DCPD could be traced to 1 h and then vanished. This result was well consistent to the SEM observations shown in Fig. 5, where sheet-like crystals were observed within the macropores just around 30 min after hydration started. Based on the solubility phase diagram of $Ca(OH)_2-H_3PO_4-H_2O$ ternary system [19], the solubility of $CaHPO_4 \cdot 2H_2O$ is lower than that of HA when $pH < 4.2$, and thus this intermediate hydration reaction product $CaHPO_4 \cdot 2H_2O$ formed in the very initial hydration time attributed to the low pH value.

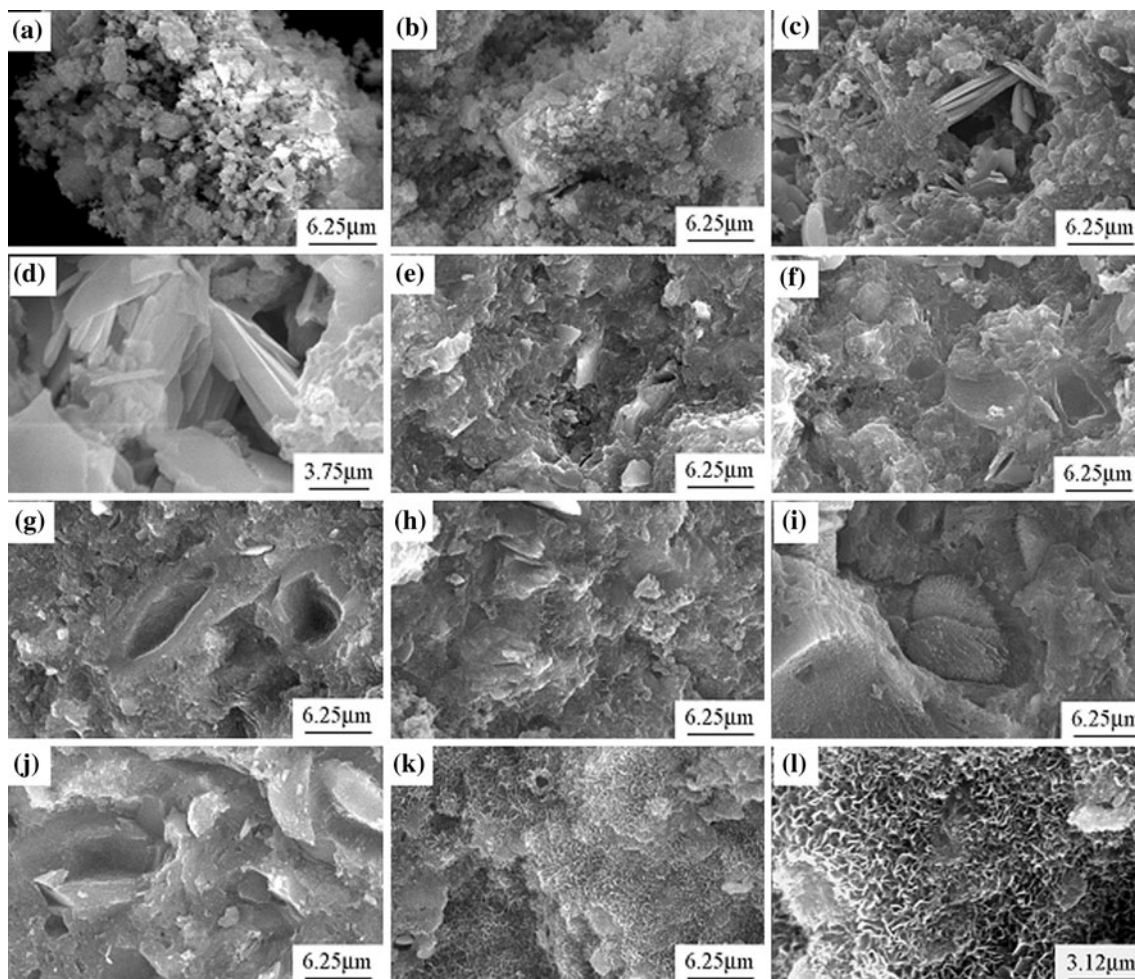


Fig. 5 SEM photographs of the $T_3S_1D_0-C_1$ powder hydrated at various hydration stages **a** 0 min; **b** 15 min; **c** and **d** 30 min; **e** 1 h; **f** 2 h; **g** 4 h; **h** 6 h; **i** 10 h; **j** 15 h; **k** and **l** 24 h

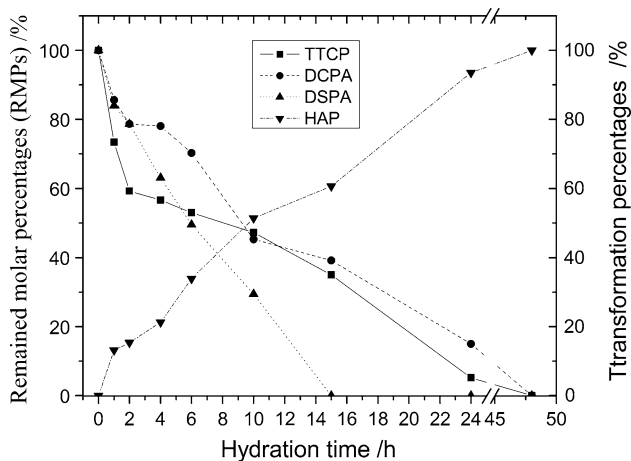
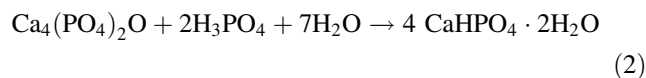
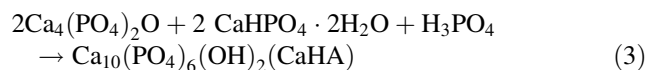


Fig. 6 The transformation percentages of the SrCaHA product and the remained molar percentages (RMPs) of respective phosphate salt reactants in the 5% SrCaHAC pastes ($T_3S_1D_0-C_1$, 1.0 M PA) at various hydration time

According to the relative results reported elsewhere [7, 20, 21], the $CaHPO_4 \cdot 2H_2O$ was mainly formed by the following hydration reaction equation (Eq. 2):



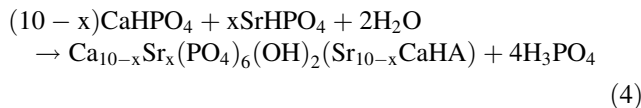
During the hydration time from 1 to 2 h, the diffraction peaks of DCPD phase basically disappeared, accompanied with a slight decrease in the diffraction peak intensity of $Ca_4(PO_4)_2O$ phase. No obvious variation happened to the diffraction peaks corresponding to the other phases, e.g. $SrHPO_4$, $CaHPO_4$. It suggested in this hydration period the DCPD phase basically hydrated into hydroxyapatite with some part of the $Ca_4(PO_4)_2O$ phase according to the following hydration reaction,



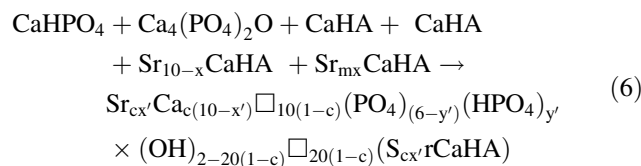
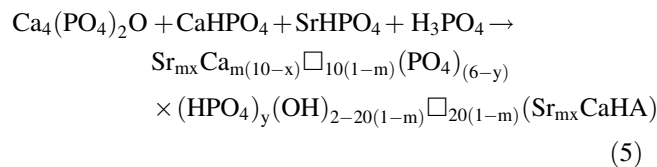
However, it seemed no identifiable diffraction peak corresponding to the hydroxyapatite phase could be

observed at 2 h, probably attributing to the low crystallinity and low amount of the hydrated hydroxyapatite phase.

From 2 to 10 h, both the diffraction peak intensities of SrHPO₄ and CaHPO₄ significantly decreased and accordingly the diffraction peak intensities of hydroxyapatite increased. However, almost no obvious variation was identified in the diffraction peaks of Ca₄(PO₄)₂O. It suggests both SrHPO₄ and CaHPO₄ transformed into Sr-containing hydroxyapatite in this period. The involved reaction was described as follows,



After 10 h, all of the diffraction peaks corresponding to the cement powder like Ca₄(PO₄)₂O, SrHPO₄, CaHPO₄ gradually decreased. SrHPO₄ phase disappeared firstly at 24 h but a minority of Ca₄(PO₄)₂O and CaHPO₄ still remained after this time. This indicates all the cement powder had been completely hydrated into hydroxyapatite phase at 48 h. The corresponding hydration reactions could be given as follows,



where, m, n, c, x, x', y, y', are the parameters related to the Sr content and weight ratio of cement powder to liquid, and □, denotes the oxygen vacancy.

In summary, the hydration mechanism of the ternary system “Ca₄(PO₄)₂O/CaHPO₄/SrHPO₄” could be understood as the following three aspects.

First, pH value was the critical kinetic factor to control the whole process of the ternary Sr-containing CPC system. The pH value testing result had ever been reported previously [4]. In the very initial hydration stage (~1 h), once the sole basic phosphoric salt Ca₄(PO₄)₂O met with the H₃PO₄, the hydration reaction rapidly started. As a result, the intermediate product CaHPO₄·2H₂O formed, accompanied with the presence of the maximal heat-liberation rate peak. This was well confirmed by the XRD pattern, SEM observation, setting time test and heat liberation behavior. In the middle hydration stage (1–2 h), Ca₄(PO₄)₂O continued to react with the intermediate

product CaHPO₄·2H₂O due to the low pH value [4]. In the later hydration stage (2–10 h), the continuous consumption of the H₃PO₄ caused the pH value of hydration system gradually increased and as a result Ca₄(PO₄)₂O almost kept no variation but both SrHPO₄ and CaHPO₄ started to hydrate. In the last hydration stage (24–48 h), attributing to the successive hydrations of SrHPO₄ and CaHPO₄, the pH value of the cement system decreased again [4] (see Eq. 4). So the remained Ca₄(PO₄)₂O completely ended its hydration at 48 h. Whatever from the heat-liberation result or the real-time XRD analysis, the identifiable hydration stages were well consistent to the pH value online testing result reported previously [4]. This is one of reasons why the H₃PO₄ is one of necessary dynamic conditions for the hydration of the Ca₄(PO₄)₂O/CaHPO₄/SrHPO₄ system cement, and why the Ca₄(PO₄)₂O/CaHPO₄/SrHPO₄ powder mixture could not be hydrated in the other PO₄³⁻-free solution, partly hydrated in the neutral PO₄³⁻-contained solution but completely hydrated in the acidic PO₄³⁻-contained solution (H₃PO₄, PA) with a concentration higher than 0.75 M reported previously [11].

Second, observed from the heat-liberation curves and the real-time XRD patterns of the ternary Sr-containing CPC system “Ca₄(PO₄)₂O/CaHPO₄/SrHPO₄”, the hydration reaction happened rapidly at the first tens of minutes and then kept gently for a long time. This suggests that the hydration reaction was controlled by the dissolving step at the very initial hydration stage and then subjected by the dispersion step at the following stages involved hours. This also agrees well with the corresponding “dissolving- dispersion” mechanism of other Sr-free CPC system reported elsewhere [16, 22].

Third, different from the other Sr-free CPC, Sr²⁺ played an important effect in the hydration of the SrCaHAC paste (see Figs. 1, 2, 3). By contrast with the 0% SrCaHAC paste under the same PA concentration, both the setting time and the latency period in hydration heat-liberation characteristic curve of the 10%SrCaHAC paste were remarkably prolonged, and the phase transformation rate of the hydration product in the 10%SrCaHAC paste was decreased. Obviously, it indicates that the present of Sr²⁺ in the cement paste significantly retards the hydration of the 10%SrCaHAC paste. This probably attributed to its higher degree of supersaturation and lower transformation rate of Sr-containing hydroxyapatite when exposed in the Sr²⁺-containing solution as compared by Sr-free HA cement paste [1]. The similar retarding effect has also been found in other high alumina cement where the pretence of silicate highly retarded the hydration of high alumina cement by promoting the formation of intermediate phase, e.g. strätlingite, and temporarily preventing the transformation of the final phase, e.g. cubic hydrogarnet (C₃AH₆) [23].

5 Conclusions

The ternary SrCaHA bone cement powder system of $\text{Ca}_4(\text{PO}_4)_2\text{O}/\text{CaHPO}_4/\text{SrHPO}_4$ exhibits an obviously different hydration characteristics compared with the conventional binary Sr-free CaHA bone cement powder system of $\text{Ca}_4(\text{PO}_4)_2\text{O}/\text{CaHPO}_4$. Among them, the PA concentration and the Sr content play outstanding roles in the hydration process of the $\text{Ca}_4(\text{PO}_4)_2\text{O}/\text{CaHPO}_4/\text{SrHPO}_4$ cement whatever from viewpoint of the very initial hydration stage or the whole hydration process. Both PO_4^{3-} and H^+ ions in PA solution attended the hydration reaction as reactants, and thus increasing the PA concentration not only promoted the dissolution of $\text{Ca}_4(\text{PO}_4)_2\text{O}$ but also pushed the hydration progress of SrCaHA bone cement. The presence of Sr^{2+} in the cement paste significantly retarded the hydration of the SrCaHA cement paste, which probably attributed to its higher degree of supersaturation for yielding apatite crystals and lower transformation rate when exposed to the Sr^{2+} -containing hydration system as compared with Sr-free CaHA cement paste. Except for the final hydration product of SrCaHA, one immediate phase, i.e. sheet-like $\text{CaHPO}_4 \cdot 2\text{H}_2\text{O}$ crystals, was also observed in the very early hydration stages (15 min–1 h), attributing to the stronger acidic hydration surroundings which accelerated the dissolution and hydration of $\text{Ca}_4(\text{PO}_4)_2\text{O}$. The probable hydration mechanism for this ternary $\text{Ca}_4(\text{PO}_4)_2\text{O}/\text{CaHPO}_4/\text{SrHPO}_4$ cement system was initially proposed, which will need to be further demonstrated by more accurate proofs.

Acknowledgments This work was supported by “the Fundamental Research Funds for the Central University”, the National Natural Science Foundation of China (No: 50702043; 51072159) and Program for New Century Excellent Talents in Universities (Chinese Ministry of Education, NCET-08-0444 (2301G107aaa)).

References

- Christoffersen J, Christoffersen MR, Kolthoff N. Effects of strontium ions on growth and dissolution of hydroxyapatite and on bone mineral detection. *Bone*. 1997;20:47–52.
- Wrong CT, Chen QZ, Lu WW, Leong JCY, Chan WK, Cheung KMC, Luk KDK. Ultrastructural study of mineralization of a strontium-containing hydroxyapatite (Sr-HA) cement in vivo. *J Biomed Mater Res*. 2004;70A:428–35.
- Xue WC, Moore JL, Hosick HL, Bose S, Bandyopadhyay A, Lu WW, Cheung KMC, Luk KDK. Osteoprecursor cell response to strontium-containing hydroxyapatite ceramics. *J Biomed Mater Res*. 2006;79A:804–14.
- Guo DG, Xu KW, Yong Han, Zhao XY. Development of a strontium-containing hydroxyapatite bone cement. *Biomaterials*. 2005;26(19):4073–83.
- Chapuy MC, Meunier PJ. Prevention and treatment of osteoporosis (see comments). *Aging (Milano)*. 1995;7:164–73.
- Roberts JT, Russell M, Kirk D, Van Rijn, Vandevivere J. Strontium 89 in Early Relapse of Hormone Treated Metastatic Prostate Cancer: Can It Delay Onset of Bone Pain. Proceedings of the 44th Annual ASTRO Meeting, 2002.
- Leroux L, Lacout JL. Preparation of calcium strontium hydroxyapatites by a new route involving calcium phosphate cements. *J Mater Res*. 2001;16(1):171–8.
- Guo YJ, Zhang M, Cehn ZQ. Property improvement by strontium ions on α -tricalcium phosphate. *Beijing J Stoma*. 2004;12(2):73–6.
- Guo DG, Xu KW, Han Yong. The influence of the Sr doses on the in vitro biocompatibility and in vivo degradability of the single-phase Sr-incorporated HAP cement. *J Biomed Mater Res*. 2008;86A:947–58.
- Wong CT, Lu WW, Chan WK, Cheung KMC, Luk KDK, Lu DS, Rabie ABM, Deng LF, Leong JCY. In vivo cancellous bone remodeling on a Strontium containing hydroxyapatite (Sr-HA) bioactive cement. *J Biomed Mater Res*. 2004;68A:513–21.
- Guo DG, Xu KW, Han Y. Preparation and characterization of a new type of Sr-containing hydroxyapatite bone cement. *Mater Sci Forum*. 2006;510–511:846–9.
- Guo DG, Xu KW, Zhao XY, Sun HL, Han Y. Research on process of strontium hydrogen phosphate synthesized by chemical wet method. *Rare Metal Mater Eng*. 2005;34(5):799–802.
- Tenhuisen KS, Brown PW. The effects of citric and acetic acids on the formation of calcium-deficient hydroxyapatite at 38°C. *J Mater Sci Mater Med*. 1994;5:291–6.
- Fukase Y, Eanes ED, Takagi S, et al. Thermal conductivity of calcium phosphate cement. *J Dent Res*. 1990;69:1852–9.
- Cao WC, Yang SS. Silicate technique [M]. Wuhan: Wuhan Technology University press; 1996. p. 69.
- Liu CS, Gai W, Pan SH, Liu ZS. The exothermal behavior in the hydration process of calcium phosphate cement. *Biomaterials*. 2003;24:2995–3003.
- Yue J, Guo DG, Xu KW, Mao TQ. Thermal stability of non-stoichiometric strontium-incorporated hydroxyapatite synthesized with a hydration process. *Rare Metal Mater Eng*. 2009;38(4):617–21.
- Takechi M, Miyamoto Y, Ishikawa K, et al. Initial histological evaluation of anti-washout type fast setting calcium phosphate cement following subcutaneous implantation. *Biomaterials*. 1998;19:2057–63.
- Brown WE, Chow LC. A new calcium phosphate, water setting cement. In: P. W. Brown, editor. *Cements Research Progress 1986*. Ohio: American Ceramic Society; 1987. p. 352–79.
- Hatim Z, Fréche M, heribeck A, Lacout JL. *Ann. Chim. (Paris)*. 1998;23:65.
- Zineb H. Thesis Institut National Polytechnique Toulouse, Tou-louse, France (1998).
- Romieu Guilhem, Garric Xavier, Munier Sylvie, Vert Michel, Boudeville Philippe. Calcium–strontium mixed phosphate as novel injectable and radio-opaque hydraulic cement. *Acta Biomater*. 2010;6:3208–15.
- Ding J, Fu Y, Beaudoin JJ. Study of hydration mechanisms in the high alumina cement–sodium silica system. *Cement and Concrete Research*. 1996;26(5):799–804.